Available online at www.sciencedirect.com
ScienceDirect
Journal of Solid State Chemistry 180 (2007) 2136–2142
JOURNAL OF SOLID STATE CHEMISTRY
www.elsevier.com/locate/jssc

Synthesis, characterization of TiO_2 nanotubes-supported MS ($TiO_2NTs@MS$, $M = Cd, Zn$) and their photocatalytic activity

Hong Li, Baolin Zhu, Yunfeng Feng, Shurong Wang, Shoumin Zhang, Weiping Huang*

Department of Chemistry, Nankai University, Tianjin 300071, PR China

Received 11 January 2007; received in revised form 29 April 2007; accepted 3 May 2007
Available online 21 May 2007

Abstract

TiO_2 nanotubes-supported MS ($TiO_2NTs@MS$, $M = Cd, Zn$) are synthesized by a simple wet chemical method at room temperature. The products are characterized with transmission electron microscopy (TEM), X-ray diffraction (XRD), UV–vis absorption spectrum and photoluminescence (PL) spectrum. Their optical and morphological properties indicate the interaction between the TiO_2 nanotube and MS nanoparticle. The photocatalytic activities of the $TiO_2NTs@MS$ are evaluated upon the oxidation of methyl orange under UV light illumination. The results reveal that the photocatalytic efficiency of the nanocomposites strongly depends on the specific interaction between MS and support.

Keywords: TiO_2 nanotubes; Metal sulfide; Photocatalytic activity; Methyl orange

1. Introduction

Titanium dioxide has been extensively employed as photocatalytic material for the purification and treatment of both contaminated air and water [1,2]. Particularly, TiO_2 in the form of nanotube is expected to have some improved properties for photocatalytic applications compared with colloidal or other forms of titania [3–7]. The tubular structure, large surface-to-volume ratio, high sedimentation rate and so on are the distinct properties of TiO_2 nanotubes, which makes TiO_2 nanotubes more suitable to be utilized as a catalyst or catalyst support for the heterogeneous catalytic reactions [4–7]. Therefore, the synthesis and characterization of TiO_2 nanotubes or modified TiO_2 nanotubes are generally studied [3–11]. In 1998, Kasuga et al. [12] developed a hydrothermal method to turn TiO_2 powders into tubular structure in 10 M NaOH solution. The synthesis process is a cheap one-step reaction, which requires neither expensive apparatus nor special chemicals. Thereby, the practical application of using TiO_2 nanotubes as photocatalyst or catalyst support is of possibility.

Though TiO_2 nanotubes have notable advances, two challenges still remain: (i) to increase the quantum yields which have remained rather low for TiO_2-based photocatalysis, and (ii) to improve the reaction selectivity to produce desired products when it is used for chemical synthesis.

To overcome the problems mentioned above, many efforts have been made to modify TiO_2 nanotubes or explore new TiO_2 nanotubes-based systems. One of the promising approaches is based on the association of TiO_2 nanotubes with other semiconductors. These nanocomposites can provide strong coupling effects, which are distinctive from the primary nanomaterials [13]. The preparations of a variety of composite materials involving TiO_2 nanotubes have been reported in literatures [13,14]. Of particular interest is a coating method to obtain one-dimensional coaxial layered TiO_2 nanotubes. The obtained materials with heterostructure exhibit improved physical and chemical properties over their single-component counterparts [15].

So far, different forms of multilayer one-dimensional coaxial nanomaterials have been produced in order to enhance or modulate their catalytic properties [15]. Among the various coaxial nanostructure nanomaterials, TiO_2

*Corresponding author.
E-mail address: huangw@eyou.com (W. Huang).

0022-4596/$ - see front matter © 2007 Elsevier Inc. All rights reserved.
doi:10.1016/j.jssc.2007.05.013

nanotubes coated with CdS [16,17] and ZnS [18] have been reported. In TiO_2NTs@CdS, the photogenerated electrons in CdS are transferred into the TiO_2 nanotubes while the holes remain in the CdS particles. This not only helps for charge separation by isolating electrons and holes in two distinct nanocrystals, but also allows the extension of the photoresponse of the photocatalyst almost in the visible region at the same time. Meanwhile, it has been well established that TiO_2NTs@ZnS composite combines the functions of both ZnS and TiO_2.

Herein, we report the synthesis of TiO_2NTs@*M*S ($M = Cd, Zn$) heterostructure nanotubes via a simple wet chemical process at room temperature and their characterization. The photocatalytic performances of the resultant nanomaterials for decomposition of methyl orange are also investigated. The experimental results indicate that the composites exhibit cooperative or synergetic effects of *M*S and the support (TiO_2 nanotubes). It is also found that the interaction between the TiO_2 nanotube and the *M*S nanoparticle greatly influences the optical and photocatalytic properties of the obtained TiO_2NTs@*M*S composites.

2. Experimental

2.1. Materials

All the reagents are analytical grade and used without any further purification.

2.2. Synthesis

2.2.1. Preparation of MS

Pure *M*S nanoparticles are prepared according to the literature [19]. Briefly, CdS suspension is prepared by mixing an appropriate amount of sulfur powder and a stoichiometric amount of $CdCl_2$ in a flask containing tetrahydrofuran (THF). After the addition of KBH_4, the suspension turns to light yellow. Finally, a yellow precipitate is formed after the mixture is stirred for 12 h at room temperature. The precipitate is collected by suction filtration and then washed several times with THF, deionized water and ethanol, successively, to remove possible impurities such as KCl, etc. For the preparation of ZnS nanoparticles, the process is the same as the above except that anhydrous $ZnCl_2$ is used instead of $CdCl_2$.

2.2.2. Preparation of TiO_2NTs@MS

The titanate nanotubes are synthesized by the method initially developed by Kasuga et al. [12], and then are calcined at 200 °C for 1 h to transform the titanate into anatase TiO_2. The TiO_2NTs@CdS samples are synthesized as follows [20]. Pure TiO_2 nanotubes, appropriate S powder and stoichiometric $CdCl_2$ are dispersed in THF (1 mg TiO_2 nanotubes/1 mL THF) by sonicating for 30 min. Then, excess KBH_4 is gradually added under vigorous stirring at ambient temperature. After the mixture is stirred for 12 h, a light yellow precipitate is formed. Then, the precipitated powder is filtered, thoroughly washed with dried THF, deionized water and ethanol. TiO_2NTs@CdS is finally obtained after the precipitate is dried in air at room temperature. Similar process is carried out to obtain white TiO_2NTs@ZnS nanocomposites. The proportions of CdS or ZnS to the total weight of catalysts are 10%, 20% and 30%.

2.3. Characterization

The samples are characterized using transmission electron microscopy (TEM, Philips T20ST) equipped with EDXA capabilities, and X-ray diffraction (XRD, diffractometer with CuKα radiation). UV–vis absorption spectra of the samples are obtained with a JASO V-570 spectrometer. Photoluminescence (PL) spectra are collected with a Sperx-F212 luminescence spectrometer.

2.4. Catalytic activity test

Photocatalytic activity experiments of the specimens used as photocatalysts for the degradation of methyl orange in water are performed in a UV-light reactor. The photocatalyst is dispersed in 100 mL methyl orange aqueous solution (17 mg/L). About 0.05 g photocatalyst is used in each experiment. The reactor is illuminated with a 300 W high-pressure mercury lamp. The concentration of methyl orange solution is monitored by measuring the absorption at 463.8 nm using a TU-1901 spectrometer. The results are corrected for the decomposition of the dye in the absence of catalysts and for adsorption of dye on the catalyst.

3. Results and discussion

3.1. Characterization of the modified TiO_2 nanotubes

XRD patterns of TiO_2 nanotubes, pure CdS, ZnS nanoparticles and their nanocomposites are displayed in Fig. 1. The TiO_2 nanotubes (Fig. 1(a)) can be indexed to an anatase TiO_2 (JCPDS No. 21-1272). In Fig. 1(b), characteristic XRD patterns of both TiO_2 and CdS nancrystals are observed. Five distinctive TiO_2 peaks are found at 25°, 38°, 48°, 55° and 63° corresponding to (101), (004), (200), (105), (211) and (204) crystal planes, respectively. Meanwhile, additional prominent peaks at angles (2θ) of 25°, 28°, 45°, 48° and 53° could be indexed to reflection from the (100), (101), (110), (103) and (112) planes of hexagonal CdS (JCPDS No. 75-1545), respectively. The sharp diffraction peaks of CdS patterns indicate that the powder has a high degree of crystallinity. Based on the Debey–Scherrer equation, the average particle size is estimated as 5 nm from the half-width of the XRD peaks.

For Fig. 1(d), except the peaks of anatase TiO_2, the residual three diffraction peaks marked ring correspond to the (111), (220) and (311) reflections of ZnS, which are completely consistent with the data of the standard card

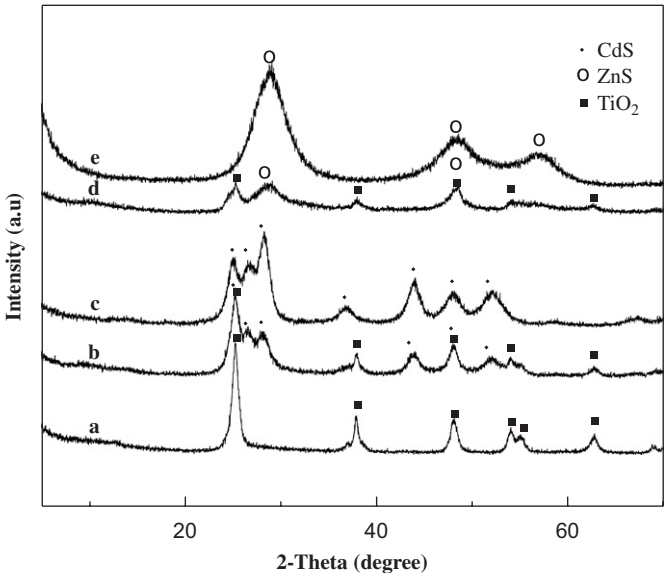

Fig. 1. XRD patterns of catalysts (a) TiO_2 nanotubes, (b) TiO_2NTs@CdS with 10 wt% CdS, (c) CdS nanoparticles, (d) TiO_2NTs@ZnS with 10 wt% ZnS and (e) ZnS nanoparticles.

(JCPDS No. 5-0566). In addition, the well-defined peaks in Figs. 1(d) and (e) indicate that the formed ZnS is of a high crystallinity. The calculated particle size of ZnS is 3 nm from XRD patterns using Debey–Scherrer formula.

Fig. 2 shows the TEM images of as-prepared titanate nanotubes and coated nanotubes with different concentrations of the precursors. The typical morphology of the as-prepared TiO_2 nanotubes is displayed in Figs. 2(a) and (b). The TEM images show that the titanate nanotubes present a smooth surface without contamination, and uniform distribution in an average diameter of 10 nm. The tubular structure remained even when they are calcinated at a temperature more than 200 °C [21]. After TiO_2 nanotubes are coated with *M*S nanoparticles, the morphologies of the TiO_2 nanotubes change greatly. Representatively, the TEM images of CdS-coated TiO_2 nanotubes are shown in Figs. 2(c) and (e). From these images, it can be seen that the amount of CdS particles on TiO_2 nanotubes varies with the concentration of formed S^{2-} ions. Figs. 2(c) and (d) display that TiO_2 nanotubes are coated with CdS nanoparticles, and partially turn into coaxial nanotubes. Fig. 2(e) shows that the TiO_2 nanotube is coated completely with CdS nanoparticles. These imply that a homogeneous coverage of TiO_2NTs@*M*S nanotubes is obtained by increasing the concentration of precursors. As shown in Fig. 2(f)–(h), the morphology properties of ZnS nanoparticles coated on the TiO_2 nanotubes are similar to that of TiO_2NTs@CdS. That is to say, discontinuously and continuously formed *M*S sheath on the TiO_2 nanotubes can be observed from the TEM images due to a multipoint growth mechanism [20]. These images demonstrate that the morphology of MS-coated TiO_2 nanotubes can be changed by adjusting the concentrations of the precursors.

Corresponding EDX analysis of TiO_2NTs@*M*S shown in Fig. 3 indicates that the chemical composition of the heterostructure nanotubes is O, Ti, S, Cd or Zn. These data clearly confirm that the products are TiO_2NTs@*M*S composite nanotubes and the *M*S coating layer has not been contaminated. Elemental analysis reveals the atomic percentages of Cd and S are 8.2 and 6.9; Zn and S are 1.9 and 1.4, respectively, which is consistent with the stoichiometric *M*S within experimental error.

Fig. 4 shows the UV–vis absorption spectra of the samples. The CdS nanoparticles (Fig. 4(b)) exhibit a well-defined absorption feature at 445 nm, which is considerably blue-shifted relative to the band gap of bulk hexagonal CdS crystals (515 nm), indicating obvious quantum size effect [19]. The absorptions of the TiO_2NTs@CdS samples (Fig. 4(c)) are shifted to 435 nm. This is in agreement with that reported by Kisch et al. The band gap of CdS employed in composite photocatalyst is shifted by an electronic semiconductor–support interaction [14]. It is found that modification of TiO_2 nanotubes with Q-CdS particles extends the optical absorption spectrum into the visible region in comparison with that of pure TiO_2 nanotubes (390 nm, Fig. 4(a)).

For ZnS (Fig. 4(d)) and TiO_2NTs@ZnS (Fig. 4(e)), absorption maximums at 310 nm are found, which are distinctly different from the bulk ZnS (340 nm) [22]. As shown in the figure, the band edge absorption of TiO_2NTs@ZnS (375 nm, Fig. 4(e)) is at longer wavelength than that of ZnS (360 nm, Fig. 4(d)), but shorter than that of TiO_2 nanotubes (405 nm, Fig. 4(a)). The red shift of band edge absorption of TiO_2NTs@ZnS can suggest that the support of TiO_2 nanotubes enhances the optical properties of ZnS considerably [18].

Fig. 5 displays the PL spectra of the CdS nanoparticles and their nanocomposites, respectively. As shown in Fig. 5(a), only an emission peak with a maximum around 435 nm has been observed in the PL spectrum pattern of CdS nanoparticles. Usually, two emissions are observed from semiconductor nanoparticles excitonic and trapped luminescence [23]. The excitonic emission is sharp and located near the absorption edge of the particles, while the trapped emission is broad and stokes-shifted. The absence of emission from trap states suggests the stoichiometric nature of CdS nanoparticles, without a surface excess of Cd^{2+} or S^{2-} vacancies.

On the other hand, since the conduction band of TiO_2 lies more positive than that of the CdS conduction band, electron injection is expected from the photoexcited CdS quantum dots (QDs) into the TiO_2 conduction band. The quenching of Q-CdS with the addition of TiO_2 must occur when Q-CdS adheres to TiO_2 nanocrystals [24]. As expected, the PL spectrum of CdS is entirely quenched for the TiO_2NTs@CdS (Fig. 5(d)), indicating efficient charge injection from the photoexcited CdS QDs into the conduction band of the TiO_2 nanotubes. The increase in quenching of emission with the increase of CdS amounts (Figs. 5(b) and (d)) clearly indicates it to be a consequence

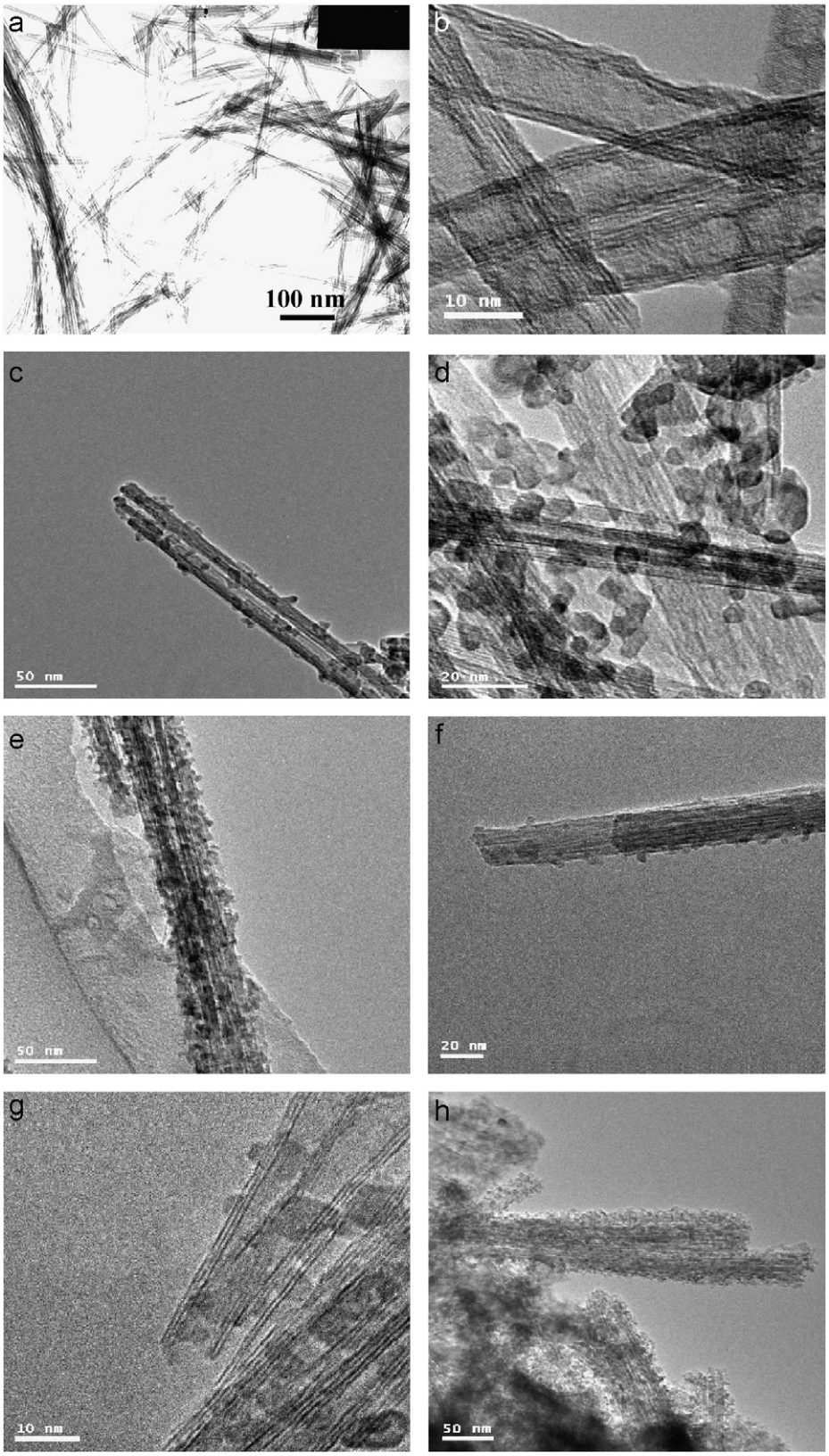

Fig. 2. TEM images of samples (a), (b) as-prepared titanate nanotubes; TiO_2NTs@CdS with different CdS concentrations (c) 10 wt%, (d) 20 wt%, (e) 30 wt%; TiO_2NTs@ZnS with various ZnS concentrations (f) 10 wt%, (g) 20 wt% and (h) 30 wt%.

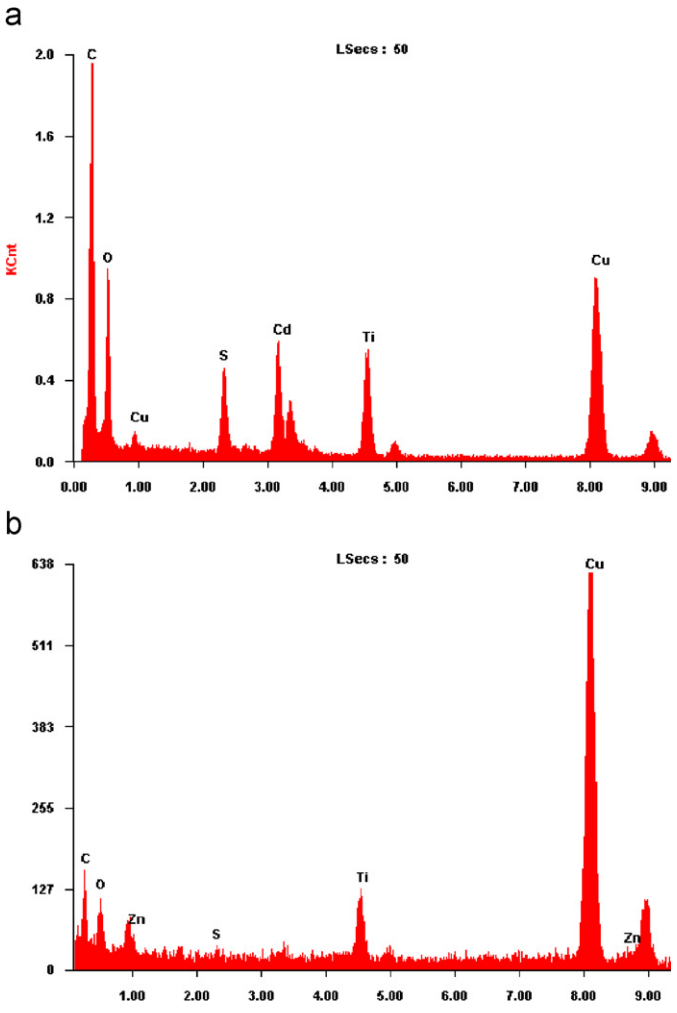

Fig. 3. EDX analysis: (a) TiO_2NTs@CdS with 10 wt% CdS and (b) TiO_2Nts@ZnS with 10 wt% ZnS.

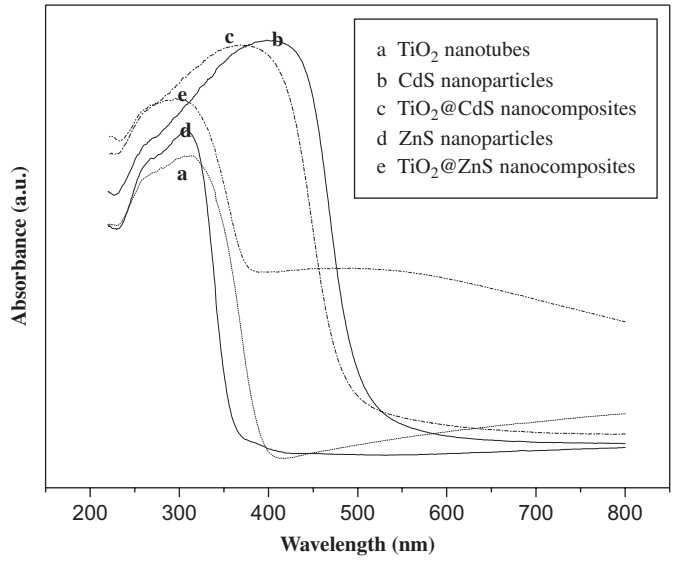

Fig. 4. UV–vis absorption spectra of (a) TiO_2 nanotubes, (b) CdS nanoparticles, (c) the TiO_2NTs@CdS with 10 wt% CdS, (d) ZnS nanoparticles and (e) TiO_2NTs@ZnS with 10 wt% ZnS.

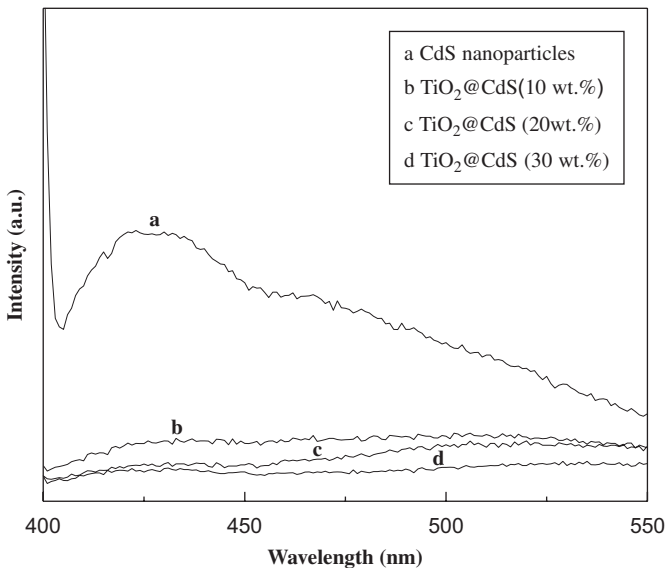

Fig. 5. PL spectra of (a) pure CdS nanoparticles, and TiO_2NTs@CdS with different concentrations of CdS (b) 10 wt%, (c) 20 wt%, and (d) 30 wt% (the excitation wavelength for the emission spectra is 375 nm).

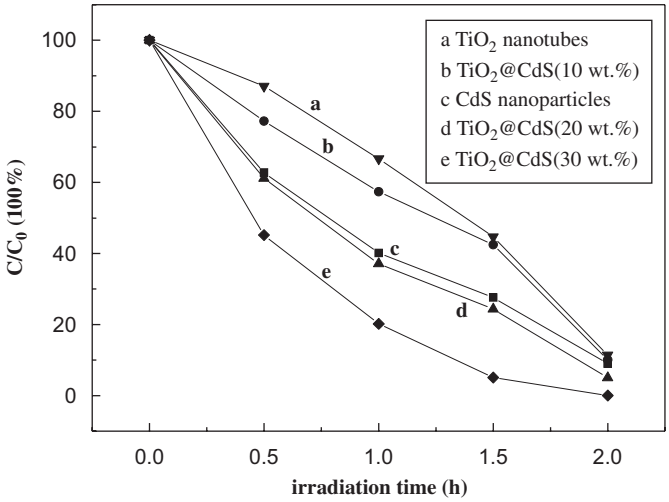

Fig. 6. Photocatalytic activities of pure TiO_2 nanotubes, CdS nanoparticles and their nanocomposites with different concentrations of CdS.

of increasing interactions between CdS and TiO_2 in the nanocomposites.

Accordingly, it can be inferred that an interaction exists between the coated metal sulfides and TiO_2 nanotube support, and the photocatalytic activity of TiO_2NTs@*M*S should be enhanced remarkably.

3.2. *Photocatalytic activity of the prepared catalysts*

Photocatalytic activities of the samples are evaluated by measuring the degradation of methyl orange in aqueous solution under UV light irradiation. Figs. 6 and 7 are two photocatalytic systems. In comparison with the uncoated TiO_2 nanotube, enhanced photocatalytic properties of the

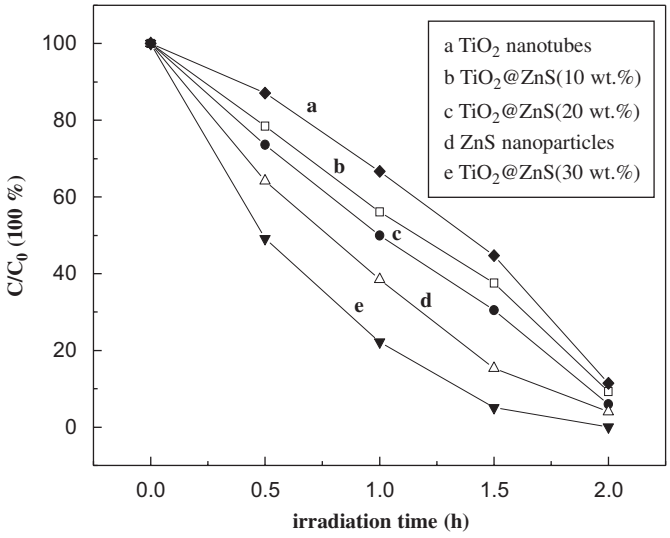

Fig. 7. Photocatalytic activities of pure TiO_2 nanotubes, ZnS nanoparticles and their nanocomposites with different concentrations of ZnS.

TiO_2NTs@*M*S heterostructure nanotubes can be observed in both Figs. 6 and 7. The improvement of the photocatalytic activity can be primarily attributed to the coupling efficiency of TiO_2 nanotubes and MS. Because the junction formed by coating *M*S on TiO_2 nanotube plays an important role in the separation of photogenerated electron–hole pair, the photocatalytic activity of TiO_2NTs@*M*S for degradation of methyl orange is found to be strongly dependent on the amount of MS. Indeed, the rates of degradations increase with the increase of *M*S content. Compared with pure TiO_2 nanotubes (Fig. 6(a)), TiO_2NTs@CdS (10 wt%, Fig. 6(b)) has higher activity. CdS absorbs UV-light and electron–hole pairs generate. The electrons injection from excited CdS into the low-lying conduction band of TiO_2 results in high concentration of electrons in conduction bands of TiO_2 nanotubes. The holes generated on TiO_2 valence band are transferred to the valence band of CdS, and consequently a high concentration of holes in valence band of the CdS nanoparticles can be created [25]. In addition, the photocatalytic activity of TiO_2NTs@CdS (20 wt%, Fig. 6(d)) has higher activity than CdS nanoparticles (Fig. 6(c)). Among the five samples, the best activity is obtained using TiO_2NTs@CdS (30 wt%) (Fig. 6(e)). It indicates that faster charge separation due to the increase of CdS content on titania contributes to the superior activity of this composite photocatalyst. This experimental result is consistent with the conclusion of Fig. 5.

As shown in Fig. 7, the highest activity is obtained using TiO_2NTs@ZnS (30 wt%, Fig. 7(e)). Due to the consequence of the ion-exchangable nature of the TiO_2 nanotubes structure, the Zn^{2+} ions surface-modified TiO_2 nanotubes facilitate the charge separation, which results in a further improvement on the photocatalytic activity for the degradation of methyl orange in water [26,27].

On the other hand, the form of the support is crucially important to obtain highly dispersed *M*S particles and photocatalysts with good performance. The large surface area and pore size of nanotubes might be beneficial for the degradation reaction involving contact of organic molecules. Meanwhile, *M*S nanoparticles have distinct catalytic functions compared with TiO_2 [28,29], which is one main factor to the improvement of the efficiency of degradation of TiO_2NTs@*M*S nanocomposites, likewise.

Based on literatures [30–32] and our experiment results, we propose a mechanism for the degradation of pollutants on TiO_2NTs@*M*S under UV light irradiation as follows:

$$M\mathrm{S}-\mathrm{TiO_2} \xrightarrow{h\nu} M\mathrm{S}(\mathrm{e^-}+\mathrm{h^+})-\mathrm{TiO_2}, \quad (1)$$

$$M\mathrm{S}(\mathrm{e^-}+\mathrm{h^+})-\mathrm{TiO_2} \rightarrow M\mathrm{S}(\mathrm{h^+})-\mathrm{TiO_2}(\mathrm{e^-}), \quad (2)$$

$$\mathrm{e^-}+\mathrm{O_2} \rightarrow \mathrm{O_2^{-\bullet}}, \quad (3)$$

$$2\mathrm{e^-}+\mathrm{O_2}+2\mathrm{H^+} \rightarrow \mathrm{H_2O_2}, \quad (4)$$

$$\mathrm{H_2O_2}+\mathrm{O_2^{-\bullet}} \rightarrow \mathrm{OH^\bullet}+\mathrm{OH^-}+\mathrm{O_2}, \quad (5)$$

$$\mathrm{OH^\bullet}+\text{methyl orange} \rightarrow \text{degradation products}. \quad (6)$$

Eq. (6) is a key process in the photo-oxidation of the adsorbed organic pollutant. It can be observed that dye concentration decrease as a function of time fits well with a first-order exponential decay curve, indicating that the photooxidation follows first-order kinetics [25,33,34]. (Its kinetics may be expressed as follows: $\ln(C_0/C) = kt$, where k is the apparent reaction rate constant, C_0 and C are the initial concentration and the reaction concentration of methyl orange, respectively.)

Furthermore, considering the property of the TiO_2 nanotubes' high sedimentation rate, TiO_2NTs@*M*S nanocomposites do not suffer the drawback of the use of nano-*M*S suspension, which is limited due to the difficulty to be separated from the slurry-type reactors. Therefore, the nanocomposites can be recycled and expected to be useful in industries.

4. Conclusion

In this paper, TiO_2NTs@*M*S heterostructure nanotubes are prepared via a simple wet chemical method at room temperature. By adjusting the concentration of precursors, the TiO_2NTs@*M*S heterostructure nanotubes with various amounts of *M*S can be achieved. In addition, the nanocomposites can exhibit higher photocatalytic activity than pure TiO_2 nanotubes or *M*S nanoparticles. It is found that the interaction between the TiO_2 nanotubes and the *M*S nanoparticles greatly influences the optical and photocatalytic properties of the TiO_2NTs@*M*S composites. The method used in this paper is of potential practical applications.

Acknowledgment

This work is supported by 973 Program (2005CB623607).

References

[1] S.Z. Chu, S. Inoue, K. Wada, D. Li, H. Haneda, S. Awatsu, J. Phys. Chem. B 107 (2003) 6586–6589.
[2] P. Raja, J. Bandara, P. Giordano, J. Kiwi, Ind. Eng. Chem. Res. 44 (2005) 8959–8967.
[3] J.C. Xu, M. Lu, X.Y. Guo, H.L. Li, J. Mol. Catal. A 226 (2005) 123–127.
[4] J.M. Macak, M. Zlamal, J. Krysa, P. Schmuki, Small 3 (2007) 300–304.
[5] A. Ghicov, J.M. Macak, H. Tsuchiya, J. Kunze, V. Haeublein, L. Frey, P. Schmuki, Nano. Lett. 6 (2006) 1080–1082.
[6] G.K. Mor, K. Shankar, M. Paulose, O.K. Varghese, NanoLett. 6 (2006) 215–218.
[7] X. Quan, S.G. Yang, X.L. Ruan, H.M. Zhao, Environ. Sci. Technol. 39 (2005) 3770–3775.
[8] M.S. Sander, M.J. Cote, W. Gu, B.M. Kile, Adv. Mater. 16 (2004) 2052–2056.
[9] Y.S. Chen, J.C. Crittendeden, S. Hackney, L. Sutter, D.W. Hand, Environ. Sci. Technol. 39 (2005) 1201–1208.
[10] S. Chen, M. Paulose, C. Ruana, G.K. Mor, O.K. Varghese, D. Kouzoudis, C.A. Grimes, J. Photoch. Photobio. A 177 (2004) 177–184.
[11] S.Z. Chu, K. Wada, S. Inoue, S. Todoroki, Chem. Mater. 14 (2002) 266–272.
[12] T. Kasuga, M. Hiramatsu, A. Hoson, Langmuir 14 (1998) 3160–3163.
[13] Q. Shen, T. Sato, M. Hashimoto, C.C. Chen, T. Toyoda, Thin Solid Films 499 (2006) 299–305.
[14] J.C. Kim, J.K. Choi, Y.B. Lee, J.H. Hong, J.I. Lee, J.W. Yang, W.I. Lee, N.H. Hur, Chem. Commun. 48 (2006) 5024–5026.
[15] J. Du, J.L. Zhang, Z.M. Liu, B.X. Han, T. Jiang, Y. Huang, Langmuir 22 (2006) 1307–1312.
[16] M.C. Hsu, I.C. Leu, Y.M. Sun, M.H. Hon, J. Cryst. Growth 285 (2005) 642–648.
[17] A. Kukovecz, M. Hodos, Z. Konya, I. Kiricsi, Chem. Phys. Lett. 411 (2005) 445–449.
[18] M.R. Kim, S.J. Ahn, D. Jang, J. Nanosci. Nanotechnol. 6 (2006) 180–184.
[19] W.Z. Wang, I. Germanenko, M.S. El-Shall, Chem. Mater. 14 (2002) 3028–3033.
[20] J. Cao, J.Z. Sun, H.Y. Li, J. Mater. Chem. 14 (2004) 1203–1206.
[21] M. Zhang, Z.S. Jin, X.Y. Guo, J.J. Yang, W. Li, X.D. Wang, Z.J. Zhang, J. Mol. Catal. A 217 (2004) 203–210.
[22] Y. Zhang, Y.D. Li, J. Phys. Chem. B 108 (2004) 17805–17811.
[23] Y.W. Wang, G.W. Meng, L.D. Zhang, C.H. Liang, J. Zhang, Chem. Mater. 14 (2002) 1773–1777.
[24] H. Matsumoto, T. Matsunaga, T. Sakata, H. Mori, H. Yoneyama, Langmuir 11 (1995) 4283–4287.
[25] Y. Bessekhouad, D. Robert, J.V. Weber, J. Photochem. Photobiol. A 163 (2004) 569–580.
[26] W.Y. Choi, A. Termin, M.R. Hoffmann, J. Phys. Chem. 98 (1994) 13669–13679.
[27] J.C. Xu, Y.L. Shi, J.E. Huang, B. Wang, H.L. Li, J. Mol. Catal. A 219 (2004) 351–355.
[28] I. Salem, Catal. Rev. Sci. Eng. 45 (2003) 205–296.
[29] G.Q. Guan, T. Kida, K. Kusakabe, K. Kimura, X.M. Fang, T.L. Ma, E. Abe, A. Yoshida, Chem. Phys. Lett. 385 (2004) 319–322.
[30] L. Wu, J.C. Yu, X.Z. Fua, J. Mol. Catal. A 244 (2006) 25–32.
[31] W.D. Wang, P. Serp, P. Kalck, J.L. Faria, J. Mol. Catal. A 235 (2005) 194–199.
[32] N. Sonperone, P. Maruthamuthu, P. Pichat, J. Photochem. Photobiol. A 85 (1995) 247–255.
[33] C. Adan, J.M. Coronado, R. Bellod, J. Soria, H. Yamaok, Appl. Catal. A 303 (2006) 199–206.
[34] Y. Gao, B.H. Chen, H.H. Li, Y.X. Ma, Mater. Chem. Phys. 80 (2003) 348–355.